ELSEVIER

A simple method for estimating frequency response corrections for eddy covariance systems

W.J. Massman*

USDA/Forest Service, Rocky Mountain Research Station, 240 West Prospect, Fort Collins, CO 80526, USA

Abstract

A simple analytical formula is developed for estimating the frequency attenuation of eddy covariance fluxes due to sensor response, path-length averaging, sensor separation, signal processing, and flux averaging periods. Although it is an approximation based on flat terrain cospectra, this analytical formula should have broader applicability than just flat-terrain providing the peak frequencies of the logarithmic cospectra are known. Comparing the integral and analytical formulations for momentum flux, heat flux, vapor flux, and closed-path and open-path CO_2 eddy covariance systems demonstrates that, except for a relatively uncommon atmospheric condition, the absolute difference between the integral and approximate correction factors is less than ± 0.06 for both stable and unstable atmospheric conditions ($0 \leq z/L \leq 2$). Because closed-path systems can have the tube entrance separated longitudinally from the sonic anemometer, a cospectral transfer function is developed for the phase shift caused by the intrinsic time constant of a first-order scalar instrument and the longitudinal separation of the mouth of the tube and the sonic anemometer. The related issues of tube lag time and other spectral transfer functions are also discussed. In general, it is suggested that the simple formula should be quite useful for experimental design and numerical correction of eddy covariance systems for frequency attenuation. Published by Elsevier Science B.V.

Keywords: Eddy covariance; Frequency response corrections; Spectral transfer functions

1. Introduction

The eddy covariance technique is now used routinely for direct measurements of surface layer fluxes of momentum, heat, and trace gases (CO_2, H_2O and O_3) between the surface and the turbulent atmosphere. This technique employs a sonic anemometer for vertical velocity fluctuations, sonic thermometry for virtual temperature fluctuations, and a scalar sensor for density fluctuations. However, all sensors display some high frequency attenuation caused by the relatively slow response of the scalar sensors (i.e. first-order

instruments often characterized by time constants of 0.1 s or greater), the spatial separation of the instruments, and line or volume averaging effects associated with sensor design. Furthermore, low frequencies are also attenuated when the flux is estimated by block averaging over a finite length of time (usually between 5 and 40 min or so, e.g. Panofsky, 1988; Kaimal et al., 1989), by high-pass recursive digital filtering (often incorporated as part of the data acquisition system, e.g. McMillen, 1988), or by linear detrending of the raw data time series (e.g. Gash and Culf, 1996; Rannik and Vesala, 1999).

Although some flux loss is inevitable with any eddy covariance system, there are a variety of methods, each having its own strength and weakness, which can be

* Fax: +1-970-498-1314.
E-mail address: wmassman@fs.fed.us (W.J. Massman).

used either to correct the measured fluxes or to min-
imize flux losses through experimental design. For
example, it is possible to correct flux measurements
in situ (e.g. Laubach and McNaughton, 1999). This
method has the advantage of being relatively free of
cospectral shape, even though it assumes cospectral
similarity between heat and water vapor fluxes. How-
ever, it requires more than one measurement of the
virtual temperature flux ($\overline{w'T_v'}$), and it does not correct
for finite acoustic path length (sonic line averaging).
In addition, because $\overline{w'T_v'}$ is the standard by which all
other scalar fluxes are corrected, this method becomes
less reliable as $\overline{w'T_v'}$ approaches zero. Other meth-
ods employ spectral transfer functions, which have
the advantage of being relatively comprehensive (e.g.,
Moore, 1986), but require a priori assumptions about
the cospectral shape. If the true cospectrum resem-
bles the assumed shape, Moore's approach (Moore,
1986) does give reasonable estimates of the correc-
tion factors (Leuning and King, 1992). However, if
the true cospectrum departs significantly from the as-
sumed shape, then the correction factor can be in error
(Laubach and McNaughton, 1999). Another possibil-
ity is to estimate a cospectrum for each block averag-
ing period by Fourier transform, correct the cospec-
trum, and then integrate the corrected cospectrum to
obtain the desired flux. This Fourier transform method
may be the best method of all because it requires the
fewest assumptions. However, it is numerically inten-
sive and, therefore, impractical for long duration ex-
periments comprised of many block averaged periods.
Finally, Horst (1997) suggested a simple analytical
alternative to Moore's comprehensive numerical ap-
proach (Moore, 1986), but, because Horst's develop-
ment focuses on the (usually) slower responding scalar
sensor, it does not include the effects of line averag-
ing, sensor separation, or the data acquisition system.

The present study, which incorporates and extends
Horst's (1997) approach develops and tests a gen-
eral analytical formula for estimating the flux loss
caused by attenuation effects associated with the sonic
anemometer, the scalar sensor, sensor separation and
design, and the data acquisition system. The initial for-
mulation of this analytical method is in terms of the flat
terrain cospectra of Kaimal et al. (1972). But, because
the approximations developed for this study result in
flux loss parameterizations that are functions of the
maximum frequency f_x of the logarithmic cospectrum,

$f\text{Co}(f)$, they can be used with cospectra that differ
from the flat terrain cospectra. Consequently, be-
cause the present methods assume a relatively smooth
cospectra they require either an in situ determination of
f_x or a reasonable parameterization for it. The primary
focus of the present study is on the most challenging
scenarios: the extremum cases for the analytical ap-
proximation, i.e. the heat flux as measured by sonic
thermometry (smallest corrections) and the closed-
path flux system (largest corrections). Nevertheless,
the approximation is also tested for momentum and
water vapor flux measurements. An additional cor-
rection term to the formal analytical approximation is
developed to improve the analytical correction factors
for the relatively infrequent situation of fluxes mea-
sured during windy, stable atmospheric conditions
using first-order scalar sensors with time constants
≥ 0.1 s.

Section 2 discusses the mathematical issues related
to this study and summarizes many of the transfer
functions used with eddy covariance. Section 3 com-
pares the eddy covariance correction factors estimated
by the simple analytical model with the complete in-
tegral formulation. The final section summarizes the
results of this study and provides suggestions and rec-
ommendations that can be drawn from it.

2. Transfer functions and mathematical development

2.1. Integral expression

The true eddy flux, $\overline{w'\beta'}$, can be represented as the
integral over frequency f of the one-sided cospectrum
$\text{Co}_{w\beta}(f)$:

$$\overline{w'\beta'} = \int_0^\infty \text{Co}_{w\beta}(f)\, \mathrm{d}f \tag{1}$$

where w' and b' are the fluctuations of vertical ve-
locity and either horizontal wind speed or scalar con-
centration. However, the measured flux, $(\overline{w'\beta'})_m$, is
usually limited by the effects of sonic line averaging,
sensor separation, block averaging when computing
the fluxes, discrete time sampling, anti-noise filters,
etc. The influence of these limitations is usually rep-
resented by multiplying the cospectrum by one or
more transfer functions:

$$(\overline{w'\beta'})_{\mathrm{m}} = \int_0^\infty H(f)\mathrm{Co}_{w\beta}(f)\,\mathrm{d}f \qquad (2)$$

where for N total transfer functions, $H(f) = \prod_{i=1}^N H_i(f)$.

Although the design of the sensors and, to a certain extent, the signal processing filters may vary from one eddy covariance system to another, there is one filter that is inescapable. It results from block averaging the fluxes over a fixed time period (Panofsky, 1988; Kaimal et al., 1989). Explicitly including this filter in Eq. (2) yields

$$(\overline{w'\beta'})_{\mathrm{m}} = \int_0^\infty \left[1 - \frac{\sin^2(\pi f T_{\mathrm{b}})}{(\pi f T_{\mathrm{b}})^2}\right] H(f)\mathrm{Co}_{w\beta}(f)\,\mathrm{d}f \qquad (3)$$

where T_{b} is the block averaging period (usually between 5 and 40 min) and $H(f)$ is now understood to be the product of the remaining transfer functions. The block averaging transfer function is in essence a high pass filter that removes low frequency components of the turbulent flux.

2.2. High pass filters

In an effort to ensure a (relatively) stationary time series, additional high pass filters are sometimes employed. These include high pass digital recursive filtering of the raw data (e.g. McMillen, 1988) or, alternatively, real time linear detrending of the raw data (Gash and Culf, 1996). Implementation of the high pass digital recursive filter uses a running mean such that $x_i' = Ax_i - Ay_{i-1} = A(x_i - x_{i-1}) + Ax_{i-1}'$ (Moore, 1986; McMillen, 1988), where the subscript i refers to the sampled datum collected at time t_i, x_i' the fluctuating (or high pass filtered) datum; x_i denotes the raw (or unfiltered) datum; y_{i-1} represents the value of the running mean at the previous time step; and A is related to the time constant of the filter (discussed below). The Fourier transform of this recursive filter yields, after some complex arithmetic, the following transfer function (e.g. Moore, 1986)

$$h_{\mathrm{r}}(\omega) = \frac{[A + A^2][1 - \cos(\omega/f_{\mathrm{s}})] + j[A - A^2][\sin(\omega/f_{\mathrm{s}})]}{1 - 2A\cos(\omega/f_{\mathrm{s}}) + A^2} \qquad (4)$$

where $\omega = 2\pi f$, f_{s} is the sampling frequency (usually between 5 and 25 Hz for eddy covariance), and

$A = \mathrm{e}^{-1/(\tau_{\mathrm{r}} f_{\mathrm{s}})}$ with τ_{r} as the filter's time constant (McMillen, 1988). McMillen's (1988) experience suggests $\tau_{\mathrm{r}} \approx 150\,\mathrm{s}$ and the mathematical analysis of Kristensen (1998) suggests that $T_{\mathrm{b}}/8 < \tau_{\mathrm{r}} < T_{\mathrm{b}}$. Results of both these studies suggest that for all reasonable choices of τ_{r} and f_{s}, $0 < 1 - A < 0.0014$, i.e. A is always less than, but very close to, 1. Therefore, for frequencies of interest the phase introduced by this type of filtering can be disregarded because it is small and affects all instrument signals equally. Consequently and with no loss of generality, the cospectral transfer function associated with the high pass digital recursive filter is taken as the real part of Eq. (4). That is

$$H_{\mathrm{r}}(\omega) \approx Re[h_{\mathrm{r}}(\omega)] = \frac{[A + A^2][1 - \cos(\omega/f_{\mathrm{s}})]}{1 - 2A\cos(\omega/f_{\mathrm{s}}) + A^2} \qquad (5)$$

Because both the individual ω' and β' time series are recursively filtered, $H_{\mathrm{r}}^2(\omega)$ is the cospectral transfer function to be used when numerically evaluating Eq. (3).

Although not directly employed in the present study, the filtering effects of a linear detrending of the flux-averaging time series is also included (see Table 1). The corresponding high pass filter is discussed by Kristensen (1998) and Rannik and Vesala (1999).

2.3. Sensor and system related transfer functions-low pass filters

All other transfer functions cause high frequency attenuation of the cospectrum because they result from the inherent design and deployment geometry of the sensors. For the sake of brevity, these transfer functions (as well as those discussed above and others that have appeared in the recent literature) are summarized in Table 1 along with the reference(s) from which they are taken. Clearly, there is some overlap between this study and Moore's (1986) study. However, there are some significant differences as well. When numerically evaluating Eq. (3) this study makes no approximation to any transfer function. Moore (1986) approximated some transfer functions so as to allow the numerical integration to be done in real time by

Table 1
Equivalent time constants for sensors and associated filters for eddy covariance systems[a]

Cause of attenuation	Reference	Equivalent time constant of a first order filter
Sonic anemometer line averaging (momentum flux)	Kaimal et al., 1968	$(l_u/2.8u)$ (horizontal) $(l_w/5.7u)$ (vertical)
Sonic anemometer line averaging (scalar flux)	Kristensen and Fitzjarrald, 1984	$(l_w/8.4u)$
Lateral separation	Kristensen and Jensen, 1979	$(l_{lat}/1.1u)$
Longitudinal separation without first order instrument, $Q_a = 0$	Hicks, 1972; Kristensen and Jensen, 1979	$(l_{lon}/1.05u)$
Longitudinal separation with first order instrument, $Q_a = 0$ $(l_{lon}^* = l_{lon} + L_t u / U_t)$	Appendix A	$(4/3)[l_{lon}^* / u(1/2(l_{lon}^*/u) + \tau_1)]^{1/2}$
Line averaging scalar sensor	Gurvich, 1962; Silverman, 1968	$l_{scalar}/4.0u$
Volume averaging right circular cylinder $0.2 \le d/l_{right} \le 2.0$	Andreas, 1981	$(0.2 + 0.4(d/l_{right}))(l_{right}/u)$
Tube attenuation		
Turbulent flow	Massman, 1991	$(\sqrt{\Lambda L_t a}/0.83U_t)$ $= (\sqrt{(\Lambda a/L_t)}/0.83)(L_t/U_t)$
Volume averaging spherical volume	Zeller et al., 1989	R/u
Butterworth anti-noise filter	Moore, 1986	$1/\pi f_s$
Low pass recursive digital filter	Goulden et al., 1997	τ_r
High pass recursive digital filter	Moore, 1986; McMillen, 1988	τ_r
High pass filtering block averaging	Kaimal et al., 1989	$T_b/2.8$
High pass filtering linear detrending	Kristensen, 1998; Rannik and Vesala, 1999	$T_b/5.3$

[a] Here the quadrature spectrum is denoted by Q_a and path length, separation distances, etc., by a subscripted l. τ_1 is the intrinsic time constant of any first-order instrument and d the diameter associated with volume averaging by a scalar instrument. The horizontal wind speed is denoted by u. L_t denotes the length of a closed-path sampling tube, a its radius, Λ is a function of the Reynolds number for tube flow, and U_t the tube flow velocity. R is the radius for spherical volume averaging by a scalar instrument. T_b denotes the block averaging period for calculating the fluxes, f_s the sampling frequency, and τ_r the time constant for digital recursive filters. The sonic anemometer is assumed to have orthogonal collocated axes. The tube lag time, L_t/U_t, is usually removed from consideration by digital time shifting. It is included here as part of the longitudinal separation effects for completeness.

the data acquisition system. Furthermore, this study incorporates two transfer functions that were not available at the time of Moore (1986). The first of these is given by Massman (1991) for tube attenuation effects associated with closed-path sensors. The second, denoted $H_{phase}(\omega)$ and derived in Appendix A, is the transfer function associated with the phase shift associated with closed-path systems. It is relevant to situations where, for example, the mouth of the sampling tube of a closed-path (first-order scalar) instrument is attached to the boom arm of the sonic anemometer, but located behind the sonic anemometer relative to the direction of the wind flow. $H_{phase}(\omega)$ is given as

$$H_{phase}(\omega) = \cos[\phi_{lon}(\omega) + \phi_t(\omega)]$$
$$-\omega\tau_\beta \sin[\phi_{lon}(\omega) + \phi_t(\omega)] \quad (6a)$$

where $\phi_{lon}(\omega)$ is the phase shift associated with the longitudinal separation between the mouth of the in-

take tube and the sonic anemometer, $\phi_t(\omega)$ is the phase shift associated with tube flow, and τ_β is the response time of the first-order instrument. Here $\phi_{lon}(\omega) = \omega l_{lon}/u$, where l_{lon} is longitudinal separation distance and u is the horizontal wind speed, and $\phi_t(\omega) = \omega L_t/U_t$, where L_t denotes tube length and U_t is the tube flow velocity. Therefore, $H_{phase}(\omega)$ can be written as

$$H_{phase}(\omega) = \cos\left[\omega\left(\frac{l_{lon}}{u} + \frac{L_t}{U_t}\right)\right]$$
$$-\omega\tau_\beta \sin\left[\omega\left(\frac{l_{lon}}{u} + \frac{L_t}{U_t}\right)\right] \quad (6b)$$

As shown by Appendix A this transfer function is a generalization of the more familiar one given by Hicks (1972) and Kristensen and Jensen (1979) [i.e. $\cos(\omega l_{lon}/u)$, Table 1], which is valid only if the scalar instrument is sufficiently fast that τ_β can be ignored and if L_t/U_t, the tube lag time, is either sufficiently

small that $\phi_t(\omega)$ can be ignored for all frequencies of importance or if (as is usually the case) the w' time series is shifted digitally in time to compensate. Because most closed path systems implement the digital time shift to remove the tube lag time effects, this study will assume that $L_t/U_t = 0$ as far as the phase shift is concerned. However, the unified treatment of the phase shift developed for this study does offer some insights into the use of the maximum correlation method for the determination of L_t/U_t (e.g., McMillen, 1988). This discussion is deferred until Section 3.2.

Assuming $L_t/U_t = 0$, Eqs. (6a) and (6b) are valid only if the separation distance is not too great. In fact, the same constraint applies to all other transfer functions shown in Table 1 that are associated with horizontal (lateral or longitudinal) separation (Lee and Black, 1994). However, it is difficult to be precise about how far is too far. For example, Laubach and McNaughton (1999) found that for both stable and unstable atmospheric conditions the transfer function developed by Kristensen and Jensen (1979) for lateral separation distances is relatively accurate for a separation of 0.25 m. Leuning et al. (1982) found that during unstable daytime conditions, increasing the lateral separation distance between the fast response temperature sensor and the sonic anemometer from 0.05 to 0.45 m reduced heat fluxes by only 3%. Mindful of these experiences and for numerical purposes only, this study therefore assumes that the maximum horizontal separation distance is 0.30 m.

In Table 1 neither attenuation effects associated with vertical displacement, nor Moore's (1986) proposed corrections for aliasing are included. To date no analytical transfer function has been developed for vertical separation effects. However, Kristensen et al. (1997) have developed numerical methods for estimating these effects and it is worth repeating their recommendation that scalar sensors be placed below the level of the sonic in order to minimize the flux loss due to vertical separation (Kristensen et al., 1997). Concerning aliasing, Horst (2000) points out that it is wrong to correct fluxes for aliasing. This is because aliasing results from digitizing (or discretely sampling) a continuous time series (Jenkins and Watts, 1968). The power present within the continuous time series at frequencies beyond the Nyquist frequency, $f_s/2$, will be aliased, but aliasing itself will neither attenuate nor amplify this power when computing the

flux or variance. Aliasing can distort the spectrum or cospectrum, but it will not influence the total flux or variance. The aliased power will simply appear to be located at frequencies below the Nyquist frequency. Consequently, aliasing need to be considered only for frequency-dependent processing of a discretely sampled time series, such as anti-noise filters or spectral analysis. It is not something that must inherently be included when estimating the correction factors associated with Eq. (3).

On the other hand, if anti-noise filters (or anti-aliasing filters as they are sometimes called) are used, they will attenuate frequencies above and below the Nyquist frequency and their influence on the fluxes should be included with other corrections. When measuring fluxes such filters are used to eliminate any common source of noise that appears in both the ω' and the β' signals. The most likely source for this type of noise is high frequency AC line noise and anti-noise filters can be quite effective at reducing it. For the present purposes anti-noise filters are not assumed to be part of the data acquisition system. However, for the sake of completeness, Table 1 includes a Butterworth anti-noise filter with its half-power point at the Nyquist frequency (e.g. Moore, 1986).

2.4. Analytical approximation

This section develops an approximation to Eq. (3) for both momentum and scalar fluxes by generalizing Horst's (1997) approach. His attenuation formula, which was derived for scalar fluxes measured with a first-order instrument, is

$$\frac{\overline{(w'\beta')}_m}{\overline{w'\beta'}} = \frac{1}{1 + (2\pi n_x \tau_\beta u/z)^\alpha} \tag{7}$$

where for $z/L \le 0$, $a = 7/8$ and $n_x = 0.085$ and for $z/L > 0$, $\alpha = 1$ and $n_x = 2.0 - 1.915/(1 + 0.5z/L)$. Here z denotes the eddy covariance measurement height, L is the Monin–Obukhov length, u the mean horizontal wind speed, and n_x represents the non-dimensional frequency ($n_x = f_x z/u$) corresponding to f_x. The simplicity Horst (1997) was able to achieve results from assuming similarity between $\overline{w'T'}$ and $\overline{w'\beta'}$ cospectra and from approximating the $\overline{w'T'}$ cospectrum (for both stable and unstable atmospheric conditions) by

$$\frac{f\mathrm{Co}_{w\beta}(f)}{\overline{w'\beta'}} = \frac{2}{\pi}\frac{f/f_x}{1 + (f/f_x)^2} \qquad (8)$$

The present study, likewise, assumes similarity between $\overline{w'T'}$, $\overline{w'T_v'}$, and $\overline{w'\beta'}$ cospectra and uses Eq. (8) to approximate the observed $\overline{w'T'}$ cospectrum. A similar approximation can be made for the $\overline{u'w'}$ cospectrum and all variance spectra as well, except that n_x and the quality of the approximation may vary somewhat with each quantity being considered. Approximating by Eq. (8) the universal flat terrain curves of Kaimal et al. (1972) as given by Kaimal and Finnigan (1994) permits the following assignment for n_x for the momentum cospectrum: $n_x = 0.079$ for $z/L \leq 0$ and $n_x = 0.079(1 + 7.9z/L)^{3/4}$ for $z/L > 0$.

In addition to approximating cospectra, this study also approximates all instrument and system response functions with their first-order equivalents as listed in Table 1. Specifically, it is assumed that any low pass transfer function can be reasonably well approximated by $1/(1 + \omega^2\tau_1^2)$ and that any high pass filter transfer function can be well approximated by $1 - (1/(1 + \omega^2\tau_1^2))$, here τ_1 is the equivalent first-order time constant as determined by matching the half power point, $f_{1/2}$, of any given transfer function, $H(\omega)$, to the half power point of the first-order filter; i.e. $\tau_1 = 1/(2\pi f_{1/2})$. Obviously, this method of approximating transfer functions will introduce some errors, the largest of which is likely to be associated with approximating $H_{\mathrm{phase}}(\omega)$. The difficulty with this transfer function is that $H_{\mathrm{phase}}(\omega)$ can be negative (Appendix B) and the first-order filter cannot capture this change of sign. This is not too serious a problem for the approximation (or for the raw eddy covariance flux estimates) if the critical frequency (ω_c) at which $H_{\mathrm{phase}}(\omega) = 0$ is well into the inertial subrange, i.e. if $\omega_c \gg 2\pi f_x$. In this case the inability of the first-order filter approximation to capture the behavior of $H_{\mathrm{phase}}(\omega)$ for $\omega \leq \omega_c$ means that the flux corrections will be slightly underestimated.

A further approximation to Eq. (3) results from combining all the high frequency filters into one equivalent first-order filter. This requires estimating an equivalent first-order time constant τ_e, for the entire set of low pass filters associated with sonic line averaging, sensor separation, finite response times etc. are shown in Table 1. One approximation for τ_e that was found to be quite adequate is

$$\tau_e = \sqrt{\sum_{i=1}^{M}\tau_i^2} \qquad (9)$$

where M is the total number of instrument filters and the τ_is are their associated equivalent first-order time constants (Table 1). The advantage that Eq. (9) has over other approaches of providing τ_e is that it automatically determines which filters contribute the most to the high frequency flux attenuation.

Incorporating these approximations into Eq. (3) and changing the variable of integration yields the following expression for the flux loss:

$$\frac{(\overline{w'\beta'})_m}{\overline{w'\beta'}} = \frac{2}{\pi}\int_0^\infty \left(\frac{1}{1 + x^2}\right)\left(\frac{a^2x^2}{1 + a^2x^2}\right)$$
$$\times \left(\frac{a^2x^2}{1 + a^2x^2}\right)\left(\frac{b^2x^2}{1 + b^2x^2}\right)\left(\frac{1}{1 + p^2x^2}\right)\,\mathrm{d}x$$
$$(10)$$

where $a = 2\pi f_x\tau_h$, $b = 2\pi f_x\tau_b$, and $p = 2\pi f_x\tau_e$ and τ_h and τ_b are the equivalent time constants associated with trend removal (τ_h) and block averaging (τ_b). The four terms of the integrand (from left to right) are the approximated cospectrum, $1/(1+x^2)$; the two high pass filters associated with trend removal, $a^2x^2/(1+a^2x^2)$; block averaging, $b^2x^2/(1+b^2x^2)$; and the approximate first-order low pass filter associated with high frequency attenuation due to instrument design and signal processing, $1/(1+p^2x^2)$. The analytical approximation to Eq. (10) is given as follows and derived in Appendix B.

$$\frac{(\overline{w'\beta'})_m}{\overline{w'\beta'}} = \left[\frac{ab}{(a+1)(b+1)}\right]\left[\frac{ab}{(a+p)(b+p)}\right]$$
$$\left[\frac{1}{(p+1)}\right]\left[1 - \frac{p}{(a+1)(a+p)}\right] \quad (11)$$

Although Eq. (11) is a reasonably precise analytical approximation to Eq. (3), comparisons to the numerical evaluation showed that Eq. (11) could be further improved. First, for unstable atmospheric conditions each of the factors a, b, and p can be raised to the power of 0.925. This slight correction to the original formulation was suggested by Horst (1997) and compensates in part for the relatively poorer approximation of the unstable cospectrum by Eq. (8). It should also be noted that the present value of 0.925 for the

exponent is used rather than Horst's original value of 0.875 because 0.925 gave slightly better agreement with Eq. (3). The second correction is most useful when deploying a first-order scalar instrument (which herein is assumed to have an intrinsic response time $\tau_\beta \geq 0.1$ s) during stable atmospheric conditions with high winds. Under these conditions f_x increases significantly and $\tau_e \to \tau_\beta$, in turn, causing Eq. (11) to progressively underestimate the true value of the integral. Again a combination of mathematical analysis and trail and error suggested that for this relatively rare situation Eq. (11) can be improved by including an additional multiplicative term:

$$\frac{1 + 0.9p}{1 + p}$$

Table 2 summarizes all the analytical approximations to Eq. (3) and the next section examines the performance of these analytical expressions. Finally, it should be reemphasized here that when evaluating the exact integral, Eq. (3), the Kaimal et al. (1972) flat terrain cospectra are used and no approximations are made to any transfer function.

3. Comparison of integral and analytical approaches

3.1. L_t/U_t phase effects have been removed by digital time shifting

Five different eddy covariance scenarios were tested for this study: momentum flux, virtual temperature flux (sonic thermometry), water vapor flux with an open path Krypton hygrometer, and both open- and closed-path CO_2 systems. This study focuses on the latter two scenarios and the sonic thermometry virtual temperature flux because they represent the extremum cases for the analytical approach and they are probably of somewhat greater interest in general. For these simulations the following assignments are made

1. the sonic anemometer has collocated vertical (l_w) and horizontal (l_u) paths of length 0.15 m; the block averaging period, T_b is 30 min; the high pass recursive time constant, τ_r, is 450 s ($=T_b/4$, after Rannik and Vesala, 1999); the sampling frequency, f_s, is 10 Hz; the measurement height above the zero plane displacement (z or z-d) is 5 m; and no anti−noise filter is applied;

2. for the closed path system, the longitudinal separation, l_{lon}, is assumed to be 0.15 m; the lateral separation l_{lat} is 0.15 m; the time constant of the CO_2 instrument τ_β, is taken to be 0.1 s; and for the purposes of calculating tube attenuation (Table 1), the tube lag time, L_t/U_t, is 2.0 s and the tube aspect ratio $\sqrt{\Lambda a/L_t}$ is 0.03, where from Massman (1991) Λ is a function of the tube flow Reynolds number and a is the tube radius;

3. for the open path system the lateral separation is 0.30 m; the CO_2 sensor path length is 0.20 m with an aspect ratio for volume averaging over a right circular cylinder (=[diameter]/[path length]) of 0.2 (Andreas, 1981); and no longitudinal separation is assumed.

Many of these parameters are intentionally chosen to be either on the lower side or high side of normal

Table 2
Recommended analytical formulae for spectral corrections to measured momentum and scalar fluxes[a]

Stable atmospheric conditions ($0 < z/L \leq 2$)	
Fast−response open path systems	$\dfrac{(\text{Flux})_m}{\text{Flux}} = \left[\dfrac{ab}{(a+1)(b+1)}\right]\left[\dfrac{ab}{(a+p)(b+p)}\right]\left[\dfrac{1}{(p+1)}\right]\left[1 - \dfrac{p}{(a+1)(a+p)}\right]$
Scalar instrument with 0.1–0.3 s response time	$\dfrac{(\text{Flux})_m}{\text{Flux}} = \left[\dfrac{ab}{(a+1)(b+1)}\right]\left[\dfrac{ab}{(a+p)(b+p)}\right]\left[\dfrac{1}{(p+1)}\right]\left[1 - \dfrac{p}{(a+1)(a+p)}\right]\left[\dfrac{1+0.9p}{1+p}\right]$
Unstable atmospheric conditions ($z/L \leq 0$) $\dfrac{(\text{Flux})_m}{\text{Flux}} = \left[\dfrac{a^\alpha b^\alpha}{(a^\alpha+1)(b^\alpha+1)}\right]\left[\dfrac{a^\alpha b^\alpha}{(a^\alpha+p^\alpha)(b^\alpha+p^\alpha)}\right]\left[\dfrac{1}{(p^\alpha+1)}\right]\left[1 - \dfrac{p^\alpha}{(a^\alpha+1)(a^\alpha+p^\alpha)}\right]$	

[a] The subscript m refers to the measured flux. Here $a = 2\pi f_x \tau_h$, $b = 2\pi f_x \tau_b$, and $p = 2\pi f_x \tau_e$. The numerical value of the exponent is dependent upon cospectral shape. For relatively broad cospectra with relatively shallow peaks, such as the flat terrain neutral/unstable flat terrain cospectrum of Kaimal et al. (1972), $\alpha = 0.925$. For sharper, more narrowly peaked cospectra, such as the stable flat terrain cospectra of Kaimal et al. (1972), $\alpha = 1$.
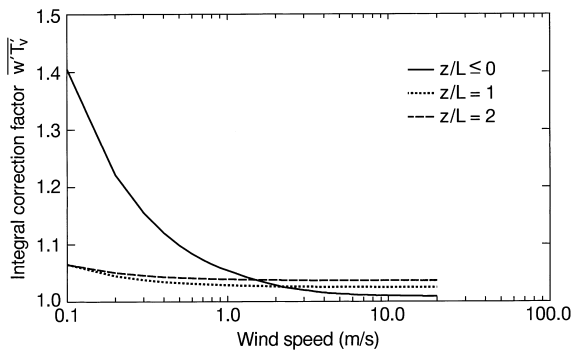
Fig. 1. Numerically integrated correction factors for $\overline{w'T_v'}$ measured using sonic thermometry. Correction factors are given for neutral and unstable atmospheric conditions (solid line, $z/L \leq 0$) and for stable conditions (dotted line, $z/L=1$; dashed line, $z/L=2$).

operating conditions or geometric factors, because this tends to produce the worst case scenarios and provides bounds on the quality of the analytical approximation.

Fig. 1 shows the correction factors, $\overline{w'T_v'}/\overline{(w'T_v')}_m \leq$, determined for three stability classes ($z/L \leq 0$ and $z/L=1$, 2) by numerical integration of Eq. (3) for the virtual temperature flux measured by sonic thermometry. (Note that the correction factor is the inverse of Eq. (3) and that throughout this study the maximum value of z/L is taken to be 2 because it is a reasonable upper limit for atmospheric observations). For wind speeds greater than 1 m/s the spectral correction factors are always less than 1.06 and the absolute difference (not shown) between the numerical integration and the analytical approximation is less than 0.01. For wind speeds less than 1 m/s and unstable conditions, the correction factor is large because as the wind speed decreases the cospectral peak f_x also decreases (Section 2.4 above). Therefore, progressively more low frequencies are attenuated at the low wind speeds due to the block averaging and detrending filters. A similar effect is noticeable during stable atmospheric conditions, but it is less pronounced because f_x is higher during stable conditions than during unstable conditions. Nevertheless, regardless of stability the analytical approximation differed from the numerical results (i.e. Fig. 1) by no more that 0.045 (absolute) at extremely low wind speeds ($u \leq 0.2$ m/s) and by less than 0.005 otherwise. (Note that throughout this study only absolute differences are discussed; the relative differences between Eqs. (3) and (11) are not partic-

ularly useful because of the nature of the application of the correction factors to the flux calculations.) A similar result was found for momentum flux, although the spectral correction factors were slightly greater than shown in Fig. 1 because sonic line averaging for scalar fluxes is less than for momentum fluxes (Table 1). The high quality performance of the analytical approach for sonic thermometry and momentum flux should not be surprising because these measurements involve sensors with relatively short time constants and relatively small characteristic length scales.

Fig. 2 shows correction factors, $\overline{w'\beta'}/\overline{(w'\beta')}_m$, as determined by numerical integration of Eq. (3) for both the open- and closed-path systems for the stability classes $z/L \leq 0$ and $z/L=1$, 2. For all cases with $u<1$ m/s, the corrections associated with the open-path system exceed the closed-path corrections. For this exceptional case, the lateral separation distance for the open-path system is dominant (and twice that of the closed-path system) so that the correction factor associated with the open-path system is slightly greater than the closed-path system. For $z/L \leq 0$ with wind speeds between 1 and 10 m s^{-1} the corrections for both systems are typically less than 1.2. However, as the atmosphere becomes more stably stratified (increasing z/L) the correction factor can become quite large and can exceed a value of 2 for the closed-path system. For
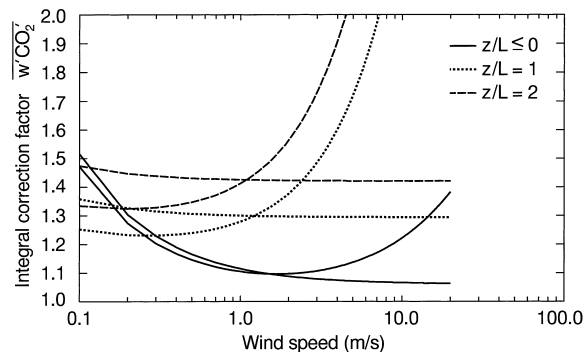

Fig. 2. Numerically integrated correction factors for open- and closed-path CO_2 eddy covariance systems. The open-path instrument is taken to be the instrument developed at NOAA/ATDD (Auble and Meyers, 1991). Correction factors are given for neutral and unstable atmospheric conditions (solid line, $z/L \leq 0$) and for stable conditions (dotted line, $z/L=1$; dashed line, $z/L=2$). Regardless of atmospheric stability, for wind speeds greater than 2 m/s the correction factor for the closed-path system exceeds that for the open-path system.

the open-path system the largest correction is slightly less than 1.5, which is probably the maximum value most researchers would be comfortable in using. In addition, it is also worth noting that for wind speeds greater than about 1 m/s the correction factor for the closed-path system increases with increasing wind speed, whereas for the open-path system they do not. Furthermore, this divergence gets progressively worse as stability increases. Leuning and Moncrieff (1990) noted the same behavior. This is a direct consequence of using a first-order system with a 'relatively large' and fixed time constant (i.e. $\tau_\beta \geq 0.1$ s). As wind speed or z/L increases f_x also increases, and as a result the low pass filtering effects associated with τ_β become progressively dominant and, in turn, they progressively attenuate more high frequencies. In the case of the open path system all time constants decrease with increasing wind speed (Table 1) compensating for the change in f_x. This is in essence why the open-path system shows virtually no wind speed dependency when $u \geq 1$ m/s. Consequently, at high wind speeds there is a compensating effect with the open-path system that does not occur with the closed-path system.

Figs. 3 and 4 show the difference between the numerically integrated corrections factors and their analytical approximations for the closed-path system. Fig. 3 does not include the additional correction term, $(1+0.9p)/(1+p)$, whereas Fig. 4 does. Because this correction term is not needed for neutral or unsta-
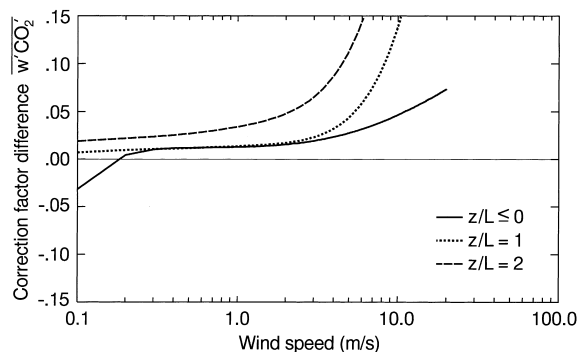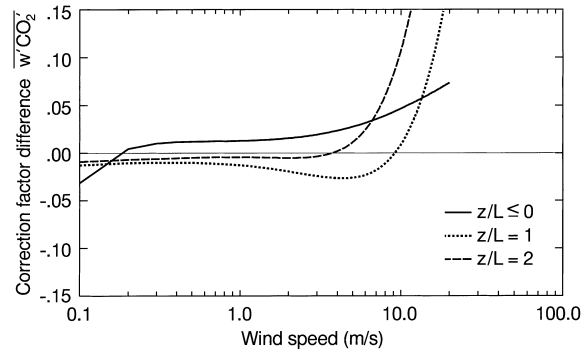

Fig. 4. Difference in the correction factors (numerical integration-analytical method) for the closed-path eddy covariance system as a function of atmospheric stability (z/L) and horizontal wind speed. The correction factor includes the additional correction term for stable atmospheric conditions with high wind speeds. The zero line is highlighted.

ble cases the $z/L \leq 0$ difference curve is the same on both figures. Comparison of these two figures clearly shows the usefulness of this additional correction factor. The overall agreement is improved particularly at wind speeds below about 10 m/s. Nevertheless, it is possible to make further improvements. For example, it is possible to parameterize this additional correction term in terms of stability or τ_β. This is because the degradation of the analytical approximation at high wind speeds and stable conditions shown in Fig. 3 gets worse as τ_β increases. Nevertheless, this is not done in the present study because the 'true' correction factor exceeds 2 and applying such a large correction factor can be done only with considerable uncertainty and skepticism. In other words, no further development of the analytical approximation seems warranted at this time.

Although not shown in this study, the analytical approximation performed very well for the open-path water vapor and CO_2 eddy covariance flux scenarios. In the water vapor case all differences were less than 0.02 (absolute) and for the CO_2 case they were less than 0.06 (absolute) for all wind speeds. The integral correction factors for the water vapor case are very similar to that shown in Fig. 2 for the open-path CO_2 case, differing only in that they are slightly smaller than for the CO_2 because the volume averaging effects are slightly smaller for the krypton hygrometer.

The approximations developed for this study are based, at least in part, on the shape of the cospectrum

Fig. 3. Difference in the correction factors (numerical integration — analytical method) for the closed-path eddy covariance system as a function of atmospheric stability (z/L) and horizontal wind speed. The correction factor does not include the additional correction term for stable atmospheric conditions with high wind speeds. The zero line is highlighted.

as a function of stability. Horst (1997) notes that the neutral/unstable $\overline{w'T'}$ cospectrum is in general somewhat broader with a shallower peak than the stable cospectrum. Interestingly the $\overline{w'CO_2'}$ cospectrum given by Anderson et al. (1986) for neutral conditions tends to peak more sharply and be less broad than the neutral/unstable $\overline{w'T'}$ cospectrum of Kaimal et al. (1972). In other words, the neutral/unstable $\overline{w'CO_2'}$ cospectrum may resemble the stable $\overline{w'T'}$ cospectrum more than the neutral/unstable $\overline{w'T'}$ cospectrum. This suggested an examination of the influence that cospectral shape may have on the analytical approximation. This sensitivity analysis was performed by numerically integrating Eq. (3) for $z/L=0$ using the more peaked stable cospectrum, rather than the broader neutral/unstable cospectrum, and then comparing how well the approximations (as given in Table 2 for the case $z/L \leq 0$) agreed with these new numerically integrated corrections. This test was performed for all five eddy covariance scenarios. In general the analytical formula overestimated the corrections for all scenarios (not shown). Except for the closed path CO_2 system, the differences were all less than 0.03 for wind speeds greater than 1 m/s, and for wind speeds less than 1 m/s the differences were all less than 0.12. For the closed path CO_2 system the differences were less than 0.05 for wind speeds greater than 0.5 m/s and less than 0.12 for lower wind speeds. These results suggest that the approximation is relatively insensitive to cospectral shape at least for a relatively smooth $z/L \leq 0$ cospectrum. Therefore, departures of (smooth) cospectrum from the flat terrain cospectral shapes presented by Kaimal and Finnigan (1994) are much less likely to cause an error in estimating the correction factor than a shift in the cospectral peak f_x away from the values they presented. For relatively 'nosier' cospectrum Laubach and McNaughton (1999) also noted the importance of f_x in determining the magnitude of the spectral corrections. By their nature the present analytical approximations capture much of the influence f_x has on the spectral corrections without being particularly sensitive to spectral shape. Nevertheless, if there is evidence or reason to believe that for any given site the cospectral shape for $z/L \leq 0$ cospectrum is peaked more sharply than suggested by the flat terrain neutral/unstable cospectrum, then the performance of the analytical approximation can be significantly improved by adjusting the 0.925

exponent (α of Table 2) back to a value of 1. This change virtually eliminated any difference between the numerical and analytical results. In other words, for more peaked $z/L \leq 0$ cospectra there is no need for a (non-unity) exponent.

Finally, a comparison between the numerical integration of Eq. (3) for the closed-path CO_2 system and Horst's (1997) approximation indicated that Horst's (1997) formula cannot be used for closed path systems. This is because the present study includes more cospectral attenuation effects than those involving a first-order scalar instrument and a sonic anemometer.

3.2. Determination of L_t/U_t for a closed path system by the maximum correlation method

For any given estimate of the flux the maximum correlation method can be used to determine the total lag time (total time shift, T_{shift}) between the w' time series and the scalar time series (e.g. Jenkins and Watts, 1968; McMillen, 1988). The flux is then corrected for the relative phase shift between the two signals by shifting one time series relative to the other by the integer part of $f_s T_{shift}$. If T_{shift} does not vary from one block averaging period to another then it is easy to include the time shift automatically as part of the on-line or real time data processing, as is often done for the tube lag time L_t/U_t. However, it is important to keep in mind that $T_{shift} \neq L_t/U_t$ and that in general T_{shift} can vary from one block averaging period to another.

For example, as discussed in Section 2.3 and Appendix A, for any given flux estimate $T_{shift}=(1/\omega)\tan^{-1}(-\omega\tau_\beta)-(l_{lon}/u)-(L_t/U_t)$. Although it is true that for a constant flow rate, the tube lag time, L_t/U_t, should remain constant for any given flux estimate, the horizontal wind speed u, can vary significantly from one block averaging period to another. To further complicate matters the longitudinal separation distance l_{lon} is a function of wind direction. For example, the present study assumes that the wind direction is basically parallel to the axis (mouth) of the sonic and that the mouth of the intake tube is located a distance l_{lon} directly behind the ω axis. However, as the wind direction rotates to 90° off axis the longitudinal separation progressively becomes a lateral separation, which is not associated with any phase or time shift. Therefore, l_{lon} is influenced by the angle between the direction of the wind and the line between the ω axis

and the mouth of the intake tube. A similar argument can be used for any lateral separation as well. Consequently, a coordinate rotation may be required to estimate l_{lon} and l_{lat} for any given block averaging period. Finally, it is not particularly obvious what influence the last term, $(1/\omega)\tan^{-1}(-\omega\tau_\beta)$, can have on any determination of T_{shift} by the maximum correlation method. In general this term is not well represented in the maximum correlation method. Therefore, in summary, any digital time shift determined with the maximum correlation method has the potential for some significant uncertainties and to vary with wind direction, wind speed, and possibly the intrinsic time constant of the instrument (which could vary with instrument performance). Consequently, it may be more insightful and accurate to study the total phase shift,

$$\phi_{shift}(\omega)=\omega T_{shift}=\tan^{-1}(-\omega\tau_\beta)-\omega(l_{lon}/u)-\omega(L_t/U_t)$$

as a function of frequency (e.g., Shaw et al., 1998) than to rely on the maximum correlation method to determine T_{shift}.

Finally there is the issue of representing the phase shift as a digital (integer) shift between the two time series because a relatively low sampling frequency can impose additional uncertainties on the flux estimates. For example, consider a closed-path system with a tube lag time of 2.1 s sampling at 5 Hz. Under this scenario, this lag time can only be represented as either 2.0 or 2.2 s. Therefore, there still remains a phase shift associated with the remaining unresolved ±0.1 s. However, the present formulation for $H_{phase}(\omega)$ could be used in conjuction with any digital time shift to correct or evaluate any uncertainty in the fluxes associated with the unresolved portion of the lag time or T_{shift}. In general therefore, given these issues concerning the phase shift, it does not seem prudent to rely solely on the maximum correlation method to determine and correct for L_t/U_t or T_{shift}.

4. Summary and recommendations

The primary purpose of this study is to develop and test an analytical approximation for estimating eddy flux corrections. In the process of attempting this goal it proved necessary to clarify some scientific aspects of making these corrections and to summarize or derive transfer functions that either had not been previously considered in the literature or have not received sufficient attention. A secondary goal is to clarify some aspects of the general methodology used for deriving transfer functions.

Results of the present study indicate that the analytical method (Tables 1 and 2) when compared with the numerical integration of Eq. (3) gave reasonable estimates of the correction factors for $0\leq z/L\leq2$ and $0.1\,\mathrm{ms}^{-1}\leq u\leq20\,\mathrm{ms}^{-1}$ for eddy covariance fluxes of momentum, virtual temperature (sonic thermometry), water vapor (open-path Krypton Hygrometer), and open- and closed-path CO_2 systems. The analytical development of these approximations also demonstrated that they improve the smaller they are and that they appear to be less sensitive to variations in spectral shape than to variations in the cospectral peak f_x. Horst (1997) reached similar conclusions. These approximations are clearly easier to employ than numerical approaches and are applicable even when fluxes are so small as to preclude the use of in situ methods. Nevertheless, the present approach is subject to the same conditions as Horst's (1997) approach, including the need for (i) a horizontally-homogeneous upwind fetch, (ii) the validity of cospectral similarity, (iii) sufficiently long averaging periods, and, preferably, (iv) relatively small corrections.

Mindful of the shortcomings, some recommendations and conclusions from this study are the following

1. For issues involving design and sensor deployment and for routine corrections to scalar and momentum eddy covariance fluxes, the results presented in Tables 1 and 2 can be recommended as reasonable substitutes for the integral method.
2. Because of the potential importance of f_x in determining the magnitude of the corrections, further scientific information and possible parameterizations of f_x, or more precisely n_x, as a function of z/L are required.
3. Given the magnitude of the corrections for stable atmospheric conditions, more research is needed on cospectrum during stable atmospheric conditions.
4. Because the present analytical approximation is fairly general it may prove useful for correcting eddy covariance measurements of velocity and scalar variances as well, although accomplishing this requires numerical testing and parameterizations of f_x or $n_x(z/L)$.

Concerning (II) and (III) above, some caution should also be noted. As Horst (1997) points out,

any determination of f_x from a typical cospectrum is difficult, first because the individual cospectral amplitudes often possess low signal-to-noise ratios, making it difficult to locate the peak cospectral frequency with any certainty, and second, distortions in the cospectrum caused by frequency dependent attenuation can shift the apparent peak to lower frequencies. Therefore, when making any eddy covariance flux measurements, researchers should give careful consideration to their methods and instrumentation when investigating cospectra and when developing transfer functions or applying any methodology for making spectral corrections. It is hoped that the present study will help in many of these considerations.

Appendix A. Derivation of the longitudinal transfer function

The complex cospectrum, $C_{\omega\beta}$, of a sonic anemometer and a first-order instrument (denoted by β) separated longitudinally (i.e. in the direction of the mean horizontal wind) by a distance l_{lon} and employing a sampling tube of length L_t is

$$C_{\omega\beta} = [h_\omega(\omega)Z_\omega][h_\beta(\omega)Z_\beta{}^*]$$
$$\times [e^{-j\omega l_{lon}/u}][e^{-j\omega\lambda_{real}L_t/U_t}] \qquad (A.1)$$

where Z_ω and Z_β are the Fourier transforms of ω' and β'; ω is the angular frequency ($=2\pi f$); u is the horizontal wind speed; λ_{real} is the real part of the first complex eigenvalue that describes spectral attenuation by tube flow (Massman, 1991); U_t is the tube flow velocity; $h_\omega(\omega)$ and $h_\beta(\omega)$ are the Fourier transforms of the instruments' filter functions; $j = \sqrt{-1}$; and the superscript * indicates complex conjugation. The first phase shift, $\omega l_{lon}/u = \phi_{lon}$, is introduced to account for longitudinal separation between the sonic anemometer and the mouth of the intake tube and is parameterized after Kristensen and Jensen (1979), who show that it

is valid providing l_{lon}/u is small compared to the mean lifetime of the eddies. The second phase shift, $\omega\lambda_{real}L_t/U_t = \phi_t$, can be immediately inferred from Eqs. (2) and (4) of Massman (1991). Although λ_{real} was not discussed by Massman (1991), it was calculated as part of his original analyses. His (1991 unpublished) results showed that $\lambda_{real}=1$ for all $\Omega \leq 10$ (where Ω is non-dimensionalized frequency, Massman, 1991) and that for $\Omega \leq 10$, λ_{real} decreases very slowly as Ω increases, which agrees with similar analyses of Barton (1983) and Chatwin (1973), and the observations and discussions of Lenschow and Raupach (1991). For the purposes of the present discussion, $\lambda_{real} \equiv 1$ can be assumed.

Substituting for the transfer function of the first-order instrument [$h_\beta(\omega)=1/(1-j\omega\tau_\beta)$, with τ_β as the time constant of β] and rearranging Eq. (A.1) yields

$$C_{\omega\beta} = \frac{h_\omega(\omega)}{(1+\omega^2\tau_\beta^2)}[\cos(\phi_{lon}+\phi_t) - j\sin(\phi_{lon}+\phi_t)]$$
$$\times [1-j\omega\tau_\beta]Z_\omega Z_\beta{}^* \qquad (A.2)$$

As discussed by Kaimal and Finnigan (1994), the real part of the cross spectrum $Z_\omega Z_\beta{}^*$ is the true cospectrum Co, and the imaginary part is the true quadrature spectrum Qa, i.e. $Z_\omega Z_\beta{}^*=$Co–jQa. Eq. (A.2) is further simplified by two important assumptions. First, it is quite reasonable to neglect the quadrature spectrum (Horst, 1997) and second, it can be assumed that the sonic anemometer does not introduce any time delay or phase shift between the ω' and β' signals for eddies larger than the path length of the sonic anemometer (Kristensen and Fitzjarrald, 1984). The first assumption allows the following substitution $Z_\omega Z_\beta{}^*=$Co. The second identifies $h_\omega(\omega)$ as a real quantity, i.e. $h_\omega(\omega)=H_\omega(\omega)$. Finally, identifying the measured cospectrum Co$_m$, as the real part of $C_{\omega\beta}$ yields

$$\text{Co}_m = H_\omega(\omega)H_\beta(\omega)[\cos(\phi_{lon}+\phi_t)$$
$$- \omega\tau_\beta\sin(\phi_{lon}+\phi_t)]\text{Co} \qquad (A.3)$$

where $H_\beta(\omega)=1/(1+\omega^2\tau_\beta^2)$. Therefore, the transfer function associated with the phase shift caused by a longitudinal separation of a first-order instrument with a sampling tube and a sonic anemometer, $H_{phase}(\omega)$, is $\cos[\omega(l_{lon}/u+L_t/U_t)] - \omega\tau_\beta \sin[\omega(l_{lon}/u+L_t/U_t)]$ as given in the text by Eq. (6b).

Finally, it should be noted that $H_{\mathrm{phase}}(\omega)$ does cause the cospectrum to change sign at high frequencies. At $\omega=0$, $H_{\mathrm{phase}}(\omega)=1$ as expected. However, as ω increases, $H_{\mathrm{phase}}(\omega)$ decreases to 0 and beyond a critical value ω_c, can become negative. This critical value is the smallest value of ω that satisfies $\cos[\omega(l_{\mathrm{lon}}/u + L_{\mathrm{t}}/U_{\mathrm{t}})] - \omega\tau_\beta\sin[\omega(l_{\mathrm{lon}}/u+L_{\mathrm{t}}/U_{\mathrm{t}})]=0$, which indicates that ω_{c} is a function of τ_β, l_{lon}/u, and $L_{\mathrm{t}}/U_{\mathrm{t}}$.

Appendix B. Development of analytical correction formula

The purpose of this appendix is to demonstrate that Eq. (11) is an approximate analytical solution to Eq. (3). As outlined in the text this is accomplished (mathematically) using three simplifications. First, all cospectra are approximated following Horst (1997). Second, the transfer function of each filter is approximated by an equivalent first-order transfer function. Third, all high frequency attenuation effects can be lumped into a single first-order transfer function. Consequently, the following expression is used to approximate Eq. (3):

$$\frac{2}{\pi}\int_0^\infty \left(\frac{1}{1+x^2}\right)\left(\frac{a^2x^2}{1+a^2x^2}\right)\left(\frac{a^2x^2}{1+a^2x^2}\right)$$
$$\times \left(\frac{b^2x^2}{1+b^2x^2}\right)\left(\frac{1}{1+p^2x^2}\right)\,\mathrm{d}x \qquad (\mathrm{B}.1)$$

where $a=2\pi f_x\tau_{\mathrm{h}}$ with τ_{h} as the equivalent time constant of the high pass filter associated with digital recursive filtering or linear detrending of the raw data time series, $b=2\pi f_x\tau_{\mathrm{b}}$ with τ_{b} as the equivalent time constant of the high pass block averaging filter, and $p=2\pi f_x\tau_{\mathrm{e}}$ with τ_{e} as the equivalent time constant of the low pass filter associated with sensor response, path length averaging, sensor separation, etc. Therefore, the first term in the integrand is the approximated cospectrum; the 'a' terms correspond to the approximated high pass filters that are associated with filters intended to insure temporal stationarity of each of the raw data time series; the 'b' term is the block averaging filter associated with the flux sampling period; and the 'p' term corresponds to the approximated effects of all high frequency sensor attenuation, e.g. $\tau_{\mathrm{e}}\leq 5$ s.

The analytical result to (B.1) is

$$\left[\frac{ab}{(a+1)(b+1)}\right]\left[\frac{ab}{(a+p)(b+p)}\right]$$
$$\times \left[\frac{1}{(p+1)}\right][F(a, b, p)] \qquad (\mathrm{B}.2)$$

where

$$F(a, b, p) = \frac{a^2}{(a+1)(a+p)}$$
$$\times \left\{1+\left(\frac{1+p}{2a}\right)\left(1+\frac{a+1}{b+a}\right)\right.$$
$$\times \left.\left(1+\frac{a+p}{b+a}\right)\right\} \qquad (\mathrm{B}.3)$$

Typical values for τ_{h}, τ_{b}, and τ_{e} allow $F(a,b,p)$ to be further simplified. Specifically, noting (from previous discussions and Table 1) that $\tau_{\mathrm{a}}\approx T_{\mathrm{b}}/5$, $\tau_{\mathrm{b}}\approx T_{\mathrm{b}}/2.8$, and $\tau_{\mathrm{e}}\ll\tau_{\mathrm{h}}$, yields $(1+((a+1)/(b+a)))(1+((a+p)/(b+a)))$ ≈ 2, which in turns can be used to simplify $F(a,b,p)$ to $1-(p/((a+1)(a+p)))$. Substituting this last expression for $F(a,b,p)$ into Eq. (B.2) yields Eq. (11) of the text.

References

Anderson, D.E., Verma, S.B., Clement, R.J., Baldocchi, D.D., Matt, D., 1986. Turbulence spectra of CO_2, water vapor, temperature and velocity over a deciduous forest, temperature and velocity over a deciduous forest. Boundary-Layer Meteorol. 38, 81–99.

Andreas, E.L., 1981. The effects of volume averaging on spectra measured with a Lyman-Alpha hygrometer. J. Appl. Meteorol. 20, 467–475.

Auble, D.L., Meyers, T.P., 1991. An open path, fast response infrared H_2O and CO_2 analyzer. In: Seventh Symposium on Meteorological Observations and Instrumentation and Special Sessions on Laser Atmospheric Studies. American Meteorological Society, Boston, pp. 30–31.

Barton, N.G., 1983. The dispersion of solute from time-dependent releases in parallel flow. J. Fluid Mech. 136, 243–267.

Chatwin, P.C., 1973. On the longitudinal dispersion of dye whose concentration varies harmonically with time. J. Fluid Mech. 58, 657–667.

Gash, J.H.C., Culf, A.D., 1996. Applying a linear detrend to eddy correlation data in real time. Boundary-Layer Meteorol. 79, 301–306.

Goulden, M.L., Daube, B.C., Fan, S.M., Sutton, D.J., Bazzazz, A., Munger, J.W., Wofsy, S.C., 1997. Physiological responses of a black spruce forest to weather. J. Geophys. Res. 102, 28987–28996.

Gurvich, A.S., 1962. The pulsation spectra of the vertical component of the wind velocity and their relations to micrometeorological conditions. Izvestiya Atmos. Oceanic Phys. 4, 101–136.

Hicks, B.B., 1972. Propellor anemometers as sensors of atmospheric turbulence. Boundary-Layer Meteorol. 3, 214–228.

Horst, T.W., 1997. A simple formula for attenuation of eddy fluxes measured with first-order response scalar sensors. Boundary-Layer Meteorol. 82, 219–233.

Horst, T.W., 2000. On frequency response corrections for eddy covariance flux measurements. Boundary-Layer Meteorol. 94, 517–520.

Jenkins, G.M., Watts, D.G., 1968. Spectral Analysis and its Application, Holden-Day, Oakland, CA, 525 pp.

Kaimal, J.C., Finnigan, J.J., 1994. Atmospheric Boundary Layer Flows — Their structure and Measurement. Oxford University Press, New York, 289 pp.

Kaimal, J.C., Wyngaard, J.C., Haugen, D.A., 1968. Spectral characteristics of surface-layer turbulence. Q. J. R. Meteorol. Soc. 98, 563–589.

Kaimal, J.C., Wyngaard, J.C., Izumi, Y., Cote, O.R., 1972. Deriving power spectra from a three-component sonic anemometer. J. Appl. Meteorol. 7, 827–837.

Kaimal, J.C., Clifford, S.F., Lataitis, R.J., 1989. Effect of finite sampling on atmospheric spectra. Boundary-Layer Meteorol. 47, 337–347.

Kristensen, L., 1998. Time Series Analysis. Dealing with Imperfect Data. Risø National Laboratory, Risø-I-1228(EN), 31 pp.

Kristensen, L., Fitzjarrald, D.R., 1984. The effect of line averaging on scalar flux measurements with a sonic anemometer near the surface, J. Atmospheric. J. Atmos. Oceanic Technol. 1, 138–146.

Kristensen, L., Jensen, N.O., 1979. Lateral coherence in isotropic turbulence and in the natural wind. Boundary-Layer Meteorol. 17, 353–373.

Kristensen, L., Mann, J., Oncley, S.P., Wyngaard, J.C., 1997. How close is close enough when measuring scalar fluxes with displaced sensors. J. Atmos. Oceanic Technol. 14, 814–821.

Laubach, J., McNaughton, K.G., 1999. A spectrum-independent procedure for correcting eddy fluxes measured with separated sensors. Boundary-Layer Meteorol. 89, 445–467.

Lee, X., Black, T.A., 1994. Relating eddy correlation sensible heat flux to horizontal sensor separation in the unstable atmospheric surface layer. J. Geophys. Res. 99, 18545–18553.

Lenschow, D.H., Raupach, M.R., 1991. The attenuation if fluctuations in scalar concentrations through sampling tubes. J. Geophys. Res. 96, 15259–15268.

Leuning, R., King, K.M., 1992. Comparison of eddy-covariance measurements of CO_2 fluxes by open- and closed-path CO_2 analysers. Boundary-Layer Meteorol. 59, 297–311.

Leuning, R., Moncrieff, J., 1990. Eddy covariance measurements using open- and closed-path CO_2 analysers: Correction for analyser water vapour sensitivity and damping fluctuations in air sampling tubes. Boundary-Layer Meteorol. 53, 63–76.

Leuning, R., Denmead, O.T., Lang, A.R.G., Ohtaki, E., 1982. Effects of heat and water vapor transport on eddy covariance measurements of CO_2 fluxes. Boundary-Layer Meteorol. 23, 209–222.

Massman, W.J., 1991. The attenuation of concentration fluctuations in turbulent flow through a tube. J. Geophys. Res. 96, 15269–15273.

McMillen, R.T., 1988. An eddy correlation technique with extended applicability to non-simple terrain. Boundary-Layer Meteorol. 43, 231–245.

Moore, C.J., 1986. Frequency response corrections for eddy correlation systems. Boundary-Layer Meteorol. 37, 17–35.

Panofsky, H.A., 1988. The effect of averaging time on velocity variances. Meteorol. Atmos. Phys. 38, 64–69.

Rannik, Ü., Vesala, T., 1999. Autoregressive filtering versus linear detrending in estimation of fluxes by the eddy covariance method. Boundary-Layer Meteorol. 91, 259–280.

Silverman, B.A., 1968. The effect of spatial averaging on spectrum estimation. J. Appl. Meteorol. 7, 168–172.

Shaw, W.J., Spicer, C.W., Kenny, D.V., 1998. Eddy correlation fluxes of trace gases using a tandem mass spectrometer. Atmos. Environ. 32, 2887–2898.

Zeller, K.F., Massman, W.J., Stocker, D., Fox, D.G., Stedman, D., Hazlett, D., 1989. Initial results from the Pawnee eddy correlation system for dry acid deposition research. USDA/Forest Service Research Paper RM-282, Rocky Mountain Forest and Range Research Station, Fort Collins, CO, 80526, USA, 30 pp.